



Originally published as:

Nickel, J., di Primio, R., Mangelsdorf, K., Stoddart, D., Kallmeyer, J. (2012): Characterisation of microbial activity in pockmark fields of the SW-Barents Sea. - *Marine Geology*, 332-334, p. 152-162.

DOI: <http://doi.org/10.1016/j.margeo.2012.02.002>

1 **Characterization of microbial activity in pockmark fields of the**
2 **SW-Barents Sea**

3 Julia C. Nickel¹, Rolando di Primio¹, Kai Mangelsdorf¹, Daniel Stoddart², Jens
4 Kallmeyer³

5 ¹ Helmholtz Centre Potsdam GFZ German Research Centre for Geosciences,
6 Telegrafenberg
7 D-14473 Potsdam, Germany, nickel@gfz-potsdam.de; kai.mangelsdorf@gfz-
8 potsdam.de

9 ² Lundin Petroleum Norway, Strandveien 50D, 1366 Lysaker, Norway;
10 daniel.stoddart@lundin-norway.no

11 ³ University of Potsdam, Karl-Liebknecht-Strasse 24, Haus 27, D-14476 Potsdam,
12 Germany; Jens.Kallmeyer@geo.uni-potsdam.de

13

14 **Keywords: Pockmark, Barents Sea, sulfate reduction, microbial activity, Loppa High.**

15 **Abstract**

16

17 Multibeam bathymetry revealed the occurrence of numerous craterlike depressions,
18 so-called pockmarks, on the sea floor of the Hammerfest Basin and the Loppa High,
19 south-western Barents Sea. To investigate whether these pockmarks are related to
20 ongoing gas seepage, microbial processes associated with methane metabolism
21 were analyzed using geochemical, biogeochemical and microbiological techniques.
22 Gravity cores were collected along transects crossing individual pockmarks, allowing
23 a direct comparison between different locations inside (assumed activity center), on
24 the rim, and outside of a pockmark (reference sites). Concentrations of hydrocarbons
25 in the sediment, particularly methane, were measured as headspace (free) gas, and
26 in the occluded and adsorbed gas fraction. Down to a depth of 2.6 m below sea floor

27 (mbsf) sulfate reduction rates were quantified by radiotracer incubations.
28 Concentrations of dissolved sulfate in the porewater were determined as well. Neither
29 the sulfate profiles nor the gas measurements show any evidence of microbial activity
30 or active fluid venting. Methane concentrations and sulfate reduction rates were
31 extremely low or even below the detection limit. The results show that the observed
32 sediment structures are most likely paleo-pockmarks, their formation probably
33 occurred during the last deglaciation.

34

35 **1 Introduction**

36 Pockmarks are craterlike depressions in the seabed that form due to expulsion of
37 fluids (Hovland and Judd, 1988). Fluids can be aqueous liquids like porewater
38 (Harrington, 1985; Whiticar, 2002) but many published examples indicate formation
39 by seeping hydrocarbons, especially methane, which can be of biogenic (Vaular et
40 al., 2010) or thermogenic origin (Gay et al., 2006; Solheim and Elverhøi, 1985).

41 Pockmarks were first discovered in the late 1960's in Nova Scotia (King and
42 MacLean, 1970), since then they have been observed globally in many different
43 geologic settings, e.g. lakes, continental slopes, shelves and rises, shallow bays,
44 fjords, as well as in the deep sea (Hovland and Judd, 1988; Judd and Hovland,
45 2007). They occur in different shapes e.g. as circular craters or as non-circular,
46 elongated forms (Hovland et al., 2002). Sizes generally range from 10 to 200 m with
47 depths up to 35 m, but also giant pockmarks with diameters of up to 1 km or more
48 have been reported (Cole et al., 2000; Ondréas et al., 2005). Pockmarks can appear
49 as single features (Prior et al., 1989) or in aggregations of hundreds of pockmarks,
50 extending over tens of square kilometers (Lammers et al., 1995).

51 Hovland and Judd (1988) proposed a general model for pockmark evolution. Gas
52 from greater depth migrates upwards through the sediment towards the seabed
53 where it accumulates and causes doming. Stretching of the seabed causes small
54 tensional fractures. Gas migrating along routes towards those fractures establishes a
55 hydraulic connection, which results in a pressure drop followed by a violent burst. A
56 unit pockmark is formed. Clusters of unit pockmarks can coalesce to a normal
57 pockmark. A model by Woolsey et al. (1975) simulating “diatreme emplacements by
58 fluidization” supports this theory. Recently, Cathles et al. (2010) came up with a
59 conceptual model of pockmark and gas chimney formation. They assume that there
60 is a capillary seal which traps the gas in the deeper sediment. Gas accumulation
61 leads to overpressure and seal failure and an upward migrating gas diapir forms.
62 With gas approaching the seabed, the sediment becomes fluidized and is removed,
63 pockmarks begin to develop.

64 Pockmark formation is often associated with tectonic or sedimentary features such as
65 faults or buried channels (Chand et al., 2008). It can be controlled by underlying
66 bedrock and lithological boundaries (Forwick et al., 2009), but can also be triggered
67 by extreme events like earthquakes and tsunamis, melting of grounded icebergs or
68 even by human influence (Hovland et al., 2002).

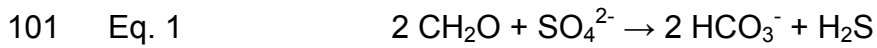
69 There are only few examples in which active fluid or gas flux could be observed.
70 However, active pockmarks have been found all over the world (Gay et al., 2007;
71 Lammers et al., 1995; Ondréas et al., 2005; Solheim and Elverhøi, 1985) but also
72 inactive, dormant pockmarks (Hovland and Judd, 1988; Ussler et al., 2003; Webb et
73 al., 2009), even entire inactive pockmark fields (Paull et al., 2002; Solheim and
74 Elverhøi, 1993) and buried paleo-pockmarks, discovered by 3D seismic data (Cole et
75 al., 2000; Hartwig et al., 2012, this issue), have been described.

76 Leakage of hydrocarbons through pockmarks infers that there is a gas source in the
77 underlying sediment. As potential indicators for deeper hydrocarbon reservoirs,
78 pockmarks received considerable interest from the hydrocarbon exploration industry
79 (Hasiotis et al., 2002; Hovland and Judd, 1988).

80 Submarine hydrocarbon seeps, such as pockmarks or mud volcanoes, are habitats
81 for specific microbial communities. Epifaunal and bacterial aggregations like
82 thiotrophic bacterial mats associated with these structures are widely described in the
83 literature (Foucher et al., 2009; Niemann et al., 2006) and provide evidence of
84 ongoing nutrient provision and metabolization. Pockmarks also play an important role
85 in the global methane cycle. Methane coming from a source at greater depth can be
86 released to the overlying ocean and even partly to the atmosphere (Lammers et al.,
87 1995; O'Connor et al., 2010; Reeburgh, 2007), effectively bypassing the zone of
88 anaerobic oxidation of methane, which normally prevents any methane escape from
89 sediments.

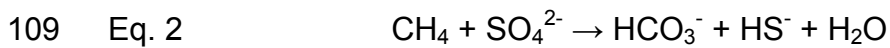
90 In subsurface sediments microbial activity dominates, with dissimilatory sulfate
91 reduction as the quantitatively most important electron acceptor process in the
92 anaerobic degradation of organic matter (D'Hondt et al., 2002; Jørgensen, 1982).
93 Thus, determination of sulfate reduction rates provides a reasonably good estimate of
94 total microbial activity in anoxic marine sediments. According to the carbon source
95 used, sulfate reduction (SR) can be divided into two main pathways.

96 Organoclastic sulfate reduction takes place in the upper part of the sediment close to
97 the sediment-water interface. It is fuelled by small organic molecules like fatty acids,
98 derived from the degradation of organic matter. The organic matter is oxidized by
99 dissolved sulfate, which is in turn reduced to hydrogen sulfide (Jørgensen, 1982;
100 Martens and Berner, 1974), according to equation 1.



102

103 Methanotrophic SR, also known as anaerobic oxidation of methane (AOM), occurs
104 below the zone of organoclastic sulfate reduction in a narrow band where there is an
105 overlap of dissolved sulfate and methane (Martens & Berner 1974, Iversen &
106 Jørgensen 1985), the so-called sulfate-methane transition zone (SMTZ). The
107 reduction of sulfate to sulfide is facilitated by the oxidation of methane to bicarbonate
108 (equation 2).



110

111 A consortium of archaea and sulfate-reducing bacteria (SRB) has been reported to
112 facilitate the anaerobic oxidation of methane with sulfate as an electron acceptor
113 (Boetius et al., 2000; Orphan et al., 2001). Recently, other electron acceptors have
114 been identified, e.g. Nitrate (Raghoebarsing et al., 2006).

115 Below the SMTZ sulfate is usually not detectable in the porewater, some very minor
116 concentrations (single to tens of μM) are usually attributed to reoxidation of hydrogen
117 sulfide during sample processing. However, molecular studies could identify sulfate
118 reducing microbes below the SMTZ (Schippers et al., 2010), even in the zone of
119 active methanogenesis (Leloup et al., 2007).

120

121 In this study, three areas in the southwestern Barents Sea were investigated (Fig. 1).
122 Two of these areas (areas B and F) are part of a large field of many small
123 depressions in the seabed (Fig. 2), which were identified as pockmarks. The third

124 area (area D) does not contain any pockmark features but was chosen for further
125 investigations due to an assumed underlying gas anomaly, as interpreted from
126 seismic data. Since pockmarks could be valuable indicators for deeper hydrocarbon
127 reservoirs, we investigated whether these pockmarks are related to ongoing gas
128 seepage or if they are manifestations of a past event. About 200 sediment gravity
129 cores were collected and analyzed. A combined study of gas measurements,
130 quantification of geochemical parameters and microbial activity was conducted to
131 obtain a better understanding about ongoing processes in and around the pockmarks
132 and to reveal their formation history.

133 **2 Geological setting**

134 The Barents Sea is a deep epicontinental sea, which borders to the Norwegian Sea
135 in the southwest and to the Arctic Ocean in the north. It is characterized by several
136 shallow banks and is crossed by deep troughs and faults (Fig. 1). The investigated
137 area is located between the southwestern part of the Loppa High, comprising the
138 Polheim sub-platform, and the Ringvassoy-Loppa Fault complex and defined by a
139 square with SW and NE coordinates $72^{\circ}13'N$, $20^{\circ}38'E$ and $71^{\circ}57'N$, $19^{\circ}53'E$ (Fig. 1).

140 The Loppa High is a structural high near the south-western margin of the Norwegian
141 Barents Sea. Fault complexes separate the Loppa High from the Hammerfest basin
142 in the southern and the Bjørnøya Basin in the western part. In the south-east it
143 passes into the Hammerfest Basin and the Bjarmeland Platform, separated by a
144 monocline.

145 The area has undergone a complex geological history, characterized by several
146 phases of uplift/subsidence and subsequent tilting and erosion (Larssen et al., 2005),
147 whereby the Loppa High is a result of Late Jurassic to Early Cretaceous tectonism

148 (Gabrielsen et al., 1990). According to Eidvin et al. (1993) and Cavanagh et al.
149 (2006) the latest erosion phase is linked to the glacial period.

150 During the Last Glacial Maximum (LGM) the study area was totally covered by
151 grounded ice (Andreassen et al., 2008; Siegert et al., 2001). During that time the ice
152 sheets reached the shelf break twice (LGM I and LGM II) in the SW-Barents Sea.
153 LGM I occurred at 19 ka followed by the Andoya Interstadial which commenced with
154 a high arctic climate after which middle to low arctic climate prevailed. Large areas of
155 the southern Barents Sea were deglaciated again. At 18 ka the LGM II occurred in
156 this area (Junttila et al., 2010; Vorren and Laberg, 1996). Between 16 and 15 ka a
157 warm spell caused the thinning of the ice sheets, triggering a major deglaciation. A
158 major drawdown of the marine-based Barents Sea Ice Sheet occurred around 14.5
159 ka. As of roughly 12 ka the study area was totally free of ice.

160

161

162 **3 Materials and Methods**

163

164 **3.1 Acoustic survey and Sampling**

165 In 2009 the Forsvarets Forskenings Institutt (FFI) conducted a multibeam bathymetric
166 survey of the Hammerfest/Loppa High and the Tromsø Basin/Ingøydjupet area of the
167 western Barents Sea region, using an EM 710 echo sounder system, with a medium
168 frequency of 70-100 kHz. During a cruise in November 2009 on R/V HU Sverdrup to
169 the Loppa High about 200 sediment gravity cores with a maximum length of 2.6 m
170 were taken in three different areas (B, D, F). Topographic seafloor maps of the three
171 investigated areas (B, D, F) showing the exact sample locations are given in

172 Figure 2. To map the general gas distribution within each area, between 15 and 115
173 cores were taken for gas analysis. Due to the massive amount of cores for gas
174 analysis, samples were only taken from the deepest part of each core. Two sediment
175 samples of ca. 500 cm³ each were taken and immediately transferred into gas-tight
176 metal cans and stored at -80°C until analysis after the cruise.

177 A total of 35 cores (exact locations are given in Table 1) were selected for detailed
178 microbiological and geochemical studies. Each of these cores was sampled in ten
179 depth intervals directly on board. To avoid contamination from shallower sediment
180 being dragged down during penetration of the core, the exterior of the material was
181 shaved off prior to subsampling.

182 Sampling for SRR incubation experiments was carried out by inserting 5-mL tip-cut
183 plastic syringes into the sediment, thereby retrieving small subcores with an intact
184 sedimentary structure. After retrieval of the subcore, the open end was closed with a
185 butyl rubber stopper and the syringes stored in nitrogen-flushed gas-tight bags in a
186 refrigerator close to in-situ temperature (+5°C). Usually this type of incubation is
187 carried out in gas-tight glass barrels. Unfortunately our glass barrels got lost during
188 transport, so we had to revert to plastic syringes. Although plastic syringes are less
189 than perfect for incubating SRR samples because of their permeability for gasses, in
190 this case the potential bias should be minimal because there is basically no methane
191 in the sample which could potentially be lost. Changes in pH due to loss of CO₂ can
192 also be neglected because the porewater is well-buffered with regard to its carbonate
193 system. An aliquot of the sediment was frozen at -20°C in N₂-flushed gas-tight bags
194 for pore-water extraction after the cruise.

195

196 **3.2 Sulfate reduction rates (SRR)**

197 Sulfate reduction rates were determined using a modification of the whole core

198 $^{35}\text{SO}_4^{2-}$ injection method (Jørgensen, 1978) as described by Ferdelman et al. (1999)

199 and Treude et al. (2005b). All incubations were performed in duplicates.

200 4 μL of carrier-free $^{35}\text{SO}_4^{2-}$ (180 kBq/ μL) were injected along the longitudinal axis of the

201 subcore. The incubations were conducted for 24 hours and terminated by transferring

202 the radiolabeled sediment into 10 mL of 20% (w/v) zinc acetate (ZnAc). Blank

203 samples were prepared by injecting $^{35}\text{SO}_4^{2-}$ radiotracer into a sample, followed by

204 immediate transfer into 20% (w/v) zinc acetate. Additionally, tracer blanks were

205 prepared by adding 4 μL of radiotracer directly into ZnAc without any sediment. The

206 total reduced inorganic sulfur (TRIS) compounds (mono- and disulfides, elemental

207 sulfur) were separated using the cold chromium distillation method (Kallmeyer et al.,

208 2004). Radioactivity was quantified using a Perkin Elmer Tri Carb 2800 TR liquid

209 scintillation analyzer and Perkin Elmer Ultima Gold XR Scintillation cocktail. SRRs

210 were calculated using the following equation (Jørgensen, 1978; Kallmeyer et al.,

211 2004):

212

213
$$\text{SRR} = \frac{a_{\text{TRIS}}}{a_{\text{TOT}}} \times \frac{[\text{SO}_4^{2-}]}{t} \times \rho_{\text{SED}} \times 1.06 \times 1000000$$

214

215 where a_{TRIS} and a_{TOT} are the activities of the TRIS compounds and the total activity

216 of the injected $^{35}\text{SO}_4^{2-}$, respectively, using the raw counts (given as counts per

217 minute, cpm) from the scintillation counter; t is the incubation time and ρ_{SED} the

218 porosity of the sediment ($\text{mL porewater cm}^{-3}$ sediment). SO_4^{2-} is seawater SO_4^{2-}

219 concentration, which was set to 28 mM for all samples, because there was no
220 measurable down-core depletion of porewater SO_4^{2-} concentrations in any of our
221 samples. 1.06 is a correction factor for the expected isotopic fractionation (Jørgensen
222 and Fenchel, 1974), 1000000 is the factor to change units from mmol L^{-1} to pmol
223 cm^{-3} .

224

225 **3.3 Determination of gas concentrations**

226 GeolabNor (Trondheim, Norway) quantified $\text{C}_1\text{-C}_6$ hydrocarbons in the headspace
227 (free) and occluded gas fraction as well as $\text{C}_1\text{-C}_8$ hydrocarbons in the adsorbed gas
228 fraction, using gas chromatography. Headspace gas was determined by thawing the
229 frozen samples over night with subsequent analysis of the free gas in the headspace
230 of the container. Occluded gas was released mechanically from an aliquot of the
231 sediment using a ball mill under vigorous shaking. Treatment of an aliquot of
232 sediment with orthophosphoric acid led to the detachment of the gas adsorbed to
233 clay minerals. All values are shown in the unit $\mu\text{mol L}^{-1}$ sediment (μM). Extrapolated
234 gas distribution maps were generated based on the obtained gas data.

235 **3.4 Porewater sulfate concentration**

236 Sediment porewater was obtained by centrifugation and careful decantation followed
237 by filtration through a $0.2\ \mu\text{m}$ membrane. Porewater sulfate concentrations were
238 determined by suppressed ion chromatography using a SYKAM IC-System (injection
239 volume $50\ \mu\text{L}$, anion exchange column, SYKAM LCA A14; conductivity detector,
240 SYKAM S3115). The elutant was a $6.25\ \text{mM}$ sodium carbonate solution with 0.1%
241 (v/v) modifier (1 mL 4-hydroxy-benzonitrile in 50 mL methanol), the flow rate was
242 $1\ \text{mL min}^{-1}$.

243

244 **4 Results**

245 **4.1 Morphology of seabed**

246 The morphology of the seabed in our study areas is shown in Figure 2. Multibeam
247 bathymetry revealed the presence of a multitude of circular seafloor depressions
248 interpreted as pockmarks. Area B and F contain an average density of 100
249 pockmarks per square kilometer, either randomly distributed or in arrays along
250 iceberg plough marks, which are the result of former iceberg activity, formed primarily
251 during glacial retreat (Solheim, 1997). The up to 15 m deep plough marks can be
252 observed all over the seabed surface.

253 The circular pockmarks are between 10 and 50 m in diameter with an average depth
254 of about 1-3 m. According to Hovland et al. (2002; 1988) these pockmarks can be
255 termed “normal pockmarks”. Additionally, some larger, irregular pockmarks with
256 diameters of up to 300 m and depths up to 25 m were observed. As mentioned
257 before, area D does not contain any pockmark features, but, like in area B and F,
258 many plough marks could be seen on the seabed of area D.

259

260 **4.2 Samples**

261 The average water depth in the investigated area was found to be around 350 m with
262 an average water temperature of about 6°C. Sediment composition appeared to be
263 very similar in all three areas, being brown to dark brown in color. Except for the first
264 10 cm which were softer, porosity averaged around 0.52 throughout the entire length
265 of the core.

266 In general the cores consisted of very sticky silty clay, occasionally containing some
267 less dense structures like small pieces of siliceous sponges as well as pebbles or
268 fragments of bivalve shells. There was no difference between sediment from within or

269 from outside the pockmarks. No hydrogen sulfide smell was noticed in any core nor
270 were there any obvious authigenic carbonate structures.

271 In area D the penetration depth of the gravity corer was relatively small (average
272 penetration depth of 50 cm). The sediment material above the anomaly structure
273 consisted of very sticky mud preventing a deeper penetration.

274

275 **4.3 Gas concentrations**

276 Concentrations of hydrocarbons (methane and higher n-alkanes, cyclic and branched
277 hydrocarbons) in the headspace (free), occluded, and adsorbed gas fraction were
278 determined on samples from the deepest interval of the core (maximum depth 2.6
279 mbsf). Extrapolated gas distribution maps were created to show the distribution of
280 hydrocarbons in the three study areas. All maps show extremely low concentrations
281 and do not reveal any correlation between gas concentration and sampling sites
282 (pockmark or reference site). The following discussion is focused just on adsorbed
283 methane, since this fraction exhibited highest concentrations. In the occluded and
284 free gas fraction only marginal amounts could be found, concentrations of longer
285 chain hydrocarbons were also negligibly low.

286 Table 2 summarizes some statistic values for the adsorbed methane and free
287 methane fraction of the three study areas. Figure 3 shows exemplarily the distribution
288 of adsorbed methane in area B. In area B the highest methane concentration in the
289 adsorbed gas fraction was 29.1 μM . Average values were only 6.19 μM in the
290 pockmark cores and 5.93 μM in reference cores (Tab. 2, Fig. 3).

291 In area D the maximum concentration of adsorbed methane was 16.84 μM , with an
292 average value of 5.42 μM . In area F concentrations of adsorbed methane reached a

293 maximum value of 19.18 μM , the average values for the pockmark samples 6.63 μM
294 and for the reference samples 5.78 μM . There are some local maxima in gas
295 concentration in all three areas, but even these anomalies are still very low and they
296 do not generally correlate to pockmarks.

297 Due to the very low gas concentrations no isotope measurements could be carried
298 out. Consequently it remains unknown whether the gas is coming from a biogenic or
299 thermogenic source.

300

301

302 **4.4 Sulfate-profiles**

303 On 12 cores porewater sulfate concentrations were determined in 10 depth intervals
304 between 0-240 cm. The profiles show very little variation with depth and among each
305 other (Fig. 4). The almost linear profiles and the only minimal decrease with depth
306 indicate very low net sulfate consumption. When extrapolating linearly, the calculated
307 SO_4^{2-} penetration depth is 37 meters, a value that is more common for oligotrophic
308 open ocean sites, not for ocean margins. For gas rich sediments, this value normally
309 ranges between 0.02 – 0.2 m (Luff and Wallmann, 2003; Treude et al., 2005a).

310

311 **4.5 Sulfate reduction rate**

312 Exemplary SRR depth profiles for pockmark and reference sites in area B are
313 presented in Figures 5a to 5d. Irrespective of pockmark or reference site, most of the
314 sulfate reduction activity was restricted to the upper 30 cm of the sediment (Figs. 5a
315 and b). In this depth interval the highest observed SRR was 600 pmol/cc/d . Deeper
316 than 30 cm below the sea floor (cmbsf) measurements fell mostly below the minimum

317 detection limit (MDL) of $10 \text{ pmol cm}^{-3} \text{ d}^{-1}$ (Fig. 5a). Only a few single samples showed
318 higher values of up to $200 \text{ pmol cm}^{-3} \text{ d}^{-1}$ (Fig. 5b), but even those maximum values
319 are still very low when compared with other sites from literature e.g. active seeps
320 (Boetius et al., 2000; Pimenov et al., 2010; Treude et al., 2003). Even in the
321 permanently cold sediments of Svalbard in the northern part of the Barents Sea,
322 sulfate reduction rates are much higher (around $60 \text{ nmol cm}^{-3} \text{ d}^{-1}$) (Finke et al., 2007).
323 In some cores all values fell below the MDL, irrespective whether the site was located
324 within or outside of a pockmark (Figs. 5c and d).

325 In area F (Figs. 5e and 5h), highest SRR was also found in the top layer. For the
326 majority of the samples, sulfate reducing activity was restricted to the upper 20 cm of
327 the sediment, reaching a maximum of up to $400 \text{ pmol cm}^{-3} \text{ d}^{-1}$ (Fig. 5f). Below this
328 depth interval most values were close or below the MDL (Fig 5g and 5h), slightly
329 higher values could only be detected in very few samples. In several cores from both
330 pockmarks and reference sites, SRR fell continuously below the MDL (Fig. 5h).

331 In area D, SRR measurements fell consistently below the minimum detection limit in
332 all samples.

333 In general, sulfate reduction rates do not show any difference between cores from
334 within or outside of pockmark structures. Profiles with slightly higher values in the
335 upper part as well as profiles showing all values below the MDL have been detected
336 for both pockmark and reference sites. Furthermore all SRR profiles show values
337 close to the detection limit, indicating a generally very low microbial activity in the
338 sediments of the investigated area.

339 **5 Discussion**

340 A multi-proxy approach was undertaken to obtain chemical, geomicrobiological and
341 geochemical evidence for active fluid or gas venting. Seafloor seeps that contain
342 methane or hydrogen sulfide can easily be identified by their sediment porewater
343 chemistry, their association with specific microbial communities and high rates of
344 microbial turnover as well as characteristic features in the seismic data. However, in
345 our study area there was no evidence for active fluid venting currently occurring from
346 either type of analysis.

347 During sampling we did not notice any hydrogen sulfide smell, not even on acidified
348 porewater samples, implying that there are neither significant amounts of dissolved
349 H₂S nor any finely precipitated sulfides such as ferrous monosulfide (FeS).

350 Furthermore, no apparent carbonate concretions, being an indicator for active or
351 recent anaerobic oxidation of methane, could be identified (Ferrell and Aharon, 1994;
352 Knittel and Boetius, 2009).

353 **5.1 Gas distribution maps**

354 Gas concentrations in sediments of the investigated areas were extremely low. In
355 some single samples, slightly elevated gas concentrations could be detected but no
356 consistent correlation with the occurrence of pockmarks or any other parameter could
357 be established. Headspace gas and occluded gas concentrations were negligibly
358 small, implying that no active seepage is taking place in the pockmark structures.
359 Highest values were always detected in the adsorbed gas fraction, it is therefore
360 reasonable to assume that this gas is derived from previous gas emissions, during
361 which a portion of the gas was adsorbed onto the clay minerals.

362 There are no significant differences between the concentrations of adsorbed
363 methane in all three areas. Throughout our study site, the average gas content is

364 very low and shows no correlation between sites from within or outside the
365 pockmarks. Very low gas contents in area D demonstrate that there is no connection
366 between the potentially underlying gas anomaly and the surface sediments. Due to
367 the fact that gas concentrations were always below saturation and no bubble
368 formation occurred, any major loss due to degassing during sampling and processing
369 can be ruled out.

370

371 **5.2 Sulfate reduction rate (SRR) & Sulfate-profiles**

372 Unlike methane, which can be lost from the sediment during coring due to degassing,
373 porewater sulfate cannot be lost as it does not form a gaseous phase. In sulfidic
374 sediments however, there is the potential for increasing sulfate concentrations due to
375 oxidation of hydrogen sulfide. Because of the lack of hydrogen sulfide, we can rule
376 out this possibility and assume the sulfate profile to represent true in-situ conditions.

377 The linear decrease in porewater sulfate concentration at all sites indicates that
378 diffusion dominates sulfate transport into the sediment and that there is no sulfate
379 consumption in this depth interval. As described by Berner (1980) SR activity can be
380 estimated from porewater sulfate profiles. However, direct radiotracer measurements
381 of SRR provide much more reliable results of SR activity, especially if diffusion is not
382 the only means of transport and other processes like advection may replenish the
383 sulfate pool in near-surface sediments (Fossing et al., 2000; Jørgensen et al., 2001;
384 Weber et al., 2001). This is the case in our study because contrary to the linear
385 sulfate profiles, which indicate no net sulfate consumption over the length of the core,
386 direct radiotracer SRR measurements reveal some very low activity in the upper few
387 cm. Much higher rates of sulfate reduction were expected in the pockmark cores,
388 particularly if active fluid venting was taking place. In most cases SR was only

389 measurable in the upper 30-40 cm below sea floor (cmbsf). This also leads to the
390 assumption, that AOM does not occur in the recovered depth interval (2.6 m) and the
391 SR-activity can be attributed entirely to organoclastic SR and not to anaerobic
392 oxidation of methane.

393 The calculated SO_4^{2-} penetration depth of 37 meter is quite deep when compared to
394 data of gas-rich sediments. In Eckernförde Bay (German Baltic Sea) for example,
395 Treude et al. (2005a) determined a penetration depth of only 0.32 m. Such a deep
396 sulfate penetration depth shows that very little sulfate is consumed in the upper part
397 of the seabed. Sulfate reduction rates in our study area are generally very low, with
398 no significant differences between SRR profiles from pockmark cores and reference
399 cores. Additionally, SRR values in area D fall consistently below the minimum
400 detection limit in all samples. This leads to the assumption that the pockmarks do not
401 release any gas at present, which is supported by our findings of very small
402 decreases in porewater sulfate concentration with sediment depth and very low gas
403 concentrations.

404

405 **5.3 Pockmark formation theory**

406 Fluid and gas venting is commonly believed to be the main factor for pockmark
407 generation. While pockmark structures could clearly be detected on the seabed, we
408 did not find any indications for significant concentrations of methane in the sediments
409 of the sampling area. Neither did we find indications for ongoing fluid flow through
410 these features.

411 Although expulsion of methane is the most frequently reported process leading to the
412 formation of pockmarks, seepage of other fluids has been described as well.

413 However, in most cases only minor quantities of gases like hydrogen sulfide or

414 carbon dioxide are associated with hydrocarbon leakage. The expulsion of porewater
415 through the seabed, so called submarine groundwater discharge (SGD), has been
416 widely described in the literature. In a review Taniguchi et al. (2002) describe
417 different systems showing SGD.

418 Some examples of pockmarks being formed by porewater discharge, have been
419 reported (Harrington, 1985; Webb et al., 2009; Whiticar and Werner, 1981). However,
420 those few examples are primarily based on assumptions and lacking direct evidence
421 of the processes involved. Moreover, the mechanisms described in these studies are
422 unable to explain the procedure of pockmark formation in detail. Given the enormous
423 area of extensive pockmark occurrence within and beyond our study area and the
424 fact that we have no evidence for past or present SGD, we rule out this mechanism.

425 Recently the occurrence of unit pockmarks (pockmarks diameter < 5 m) was
426 discussed to be an indicator for active gas seepage (Cathles et al., 2010; Hovland et
427 al., 2010).

428 Mapping unit pockmarks requires application of high-resolution bathymetry (at least
429 1m x 1m gridding) (Hovland et al., 2010). The resolution of the bathymetry equipment
430 which was used in this study is too low to locate unit pockmarks. However, due to the
431 very low gas concentrations in the pockmark as well as in the reference sites (table
432 2) we rule out the existence of seeping hydrocarbons in our study area.

433 Pockmark structures which are present in the seabed consistently over several years
434 are not necessarily an indicator for active fluid flow (Brothers et al., 2011). Numerical
435 modeling by Hammer et al. (2009) showed that upwelling currents can be a possible
436 mechanism to maintain pockmark structures even if activity has ceased for several
437 years.

438 This leads us to the more likely hypothesis that the pockmarks in our study area are
439 preserved features from past activity. The present seabed shows many plough
440 marks, derived from iceberg drifting during the last deglaciation. As undisturbed
441 pockmark craters can be found within and outside of the plough mark structures, the
442 pockmarks must have formed during and after the main phase of iceberg movement.

443 Considering the glacial history of the Barents Sea as well as the great number of
444 glacial plough marks in the study area, it can be assumed that the whole area was
445 covered by a grounded ice sheet during Last Glacial Maximum (ca. 20 ka ago).

446 Gaseous hydrocarbons like methane, derived from a deeper lying source, could have
447 migrated through the porous sediment towards near-seabed sediments. Due to the
448 conditions during the glacial period, including pressure of a thick grounded ice sheet
449 affecting the sediment, combined with the prevailing low temperatures, the necessary
450 conditions for clathrate formation were given (Kvenvolden, 1998; Sloan, 2003).

451 Methane could thus have been trapped as gas hydrate in the shallow sediment.

452 The uplifted Atlantic margin basins, comprising the Hammerfest Basin and the Loppa
453 High, contain several oil and gas fields commonly occurring in underfilled traps.
454 Corcoran and Doré (2002) suggested that this was caused due to large scale
455 leakage of gas during the Cenozoic exhumation. 2D basin modeling of this area by
456 Cavanagh et al. (2006) revealed that glacially controlled pressure oscillations provide
457 a mechanism for episodic discharge of methane from the deep petroleum reservoirs
458 and sequestration of methane as gas hydrates near the surface.

459 Alternatively sub-glacial gas hydrates may have been fed by a biogenic source or a
460 combination of biogenic and thermogenic gases.

461 About 14 ka ago the climatic conditions of the SW Barents Sea changed within a
462 relatively short time interval (approx. 5000 years, Elverhøi *et al.*, 1995), causing
463 deglaciation, melting of the ice sheet and iceberg calving. Thus, the conditions to
464 preserve hydrate layers no longer persisted, resulting in the rapid decomposition of
465 the gas hydrate as well as the release of potentially accumulated gas. Such an event
466 probably occurred over large areas of the Barents Sea more or less simultaneously,
467 resulting in widespread pockmark structures on the seabed. Similar formation
468 mechanisms have already been described for other areas (Davy *et al.*, 2010; Long,
469 1992; Long *et al.*, 1998; Mienert *et al.*, 1998; Plaza-Faverola *et al.*, 2012; Solheim
470 and Elverhøi, 1993; Sultan *et al.*, 2010).

471 Maslin *et al.* (2004) collected published data from submarine sediment failures and
472 correlated them with climatic changes from the past 45 ka. They found that over 70%
473 of continental slope failures could be dated to the periods between 15-13 ka and 11-
474 8 ka. These dates, as well as the rising sea level and global atmospheric methane
475 records, correlate well with the timing of the last deglaciation. The hypothesis of
476 pockmark formation due to rapid methane release caused by destabilization of gas
477 hydrates during this time is supported by ice-core data (Chappellaz *et al.*, 1993).

478 From the above discussion we can summarize the following points concerning the
479 proposed scenario on the formation of the Loppa High pockmarks:

- 480 1. During LGM a grounded ice sheet existed in the study area. Thermogenic and
481 / or biogenic gas from a source in the Mesozoic bedrock migrated through the
482 sediment and accumulated as gas hydrate, which was stable under the given
483 pressure and temperature conditions(Fig. 6 a).

- 484 2. The retreat of the ice sheet during deglaciation caused changes of pressure
485 conditions, which resulted in the decomposition of the hydrate layer and the
486 release of large volumes of gas over a large areal extent, resulting in the
487 formation of seafloor pockmarks (Fig. 6 b).
- 488 3. Nowadays the pockmark structures are still preserved despite the seeping
489 activity having ceased several thousand years ago (Fig. 6 c).

490 The depressions seem to be relatively young features. As many pockmarks are
491 located inside the iceberg plow marks, it can be assumed that the pockmarks were
492 formed postglacially, probably in an early phase after the last deglaciation. Similar
493 observations have also been reported from the northern Barents Sea (Solheim and
494 Elverhøi, 1993) and could be an indication for a large methane release event caused
495 by the decay of the Barents ice sheet during the last deglaciation.

496 **6 Conclusions**

497 Deep, craterlike structures, identified as pockmarks were observed by multibeam
498 bathymetry on the seafloor of the SW-Loppa High in the SW-Barents Sea.
499 Geochemical, biogeochemical and microbiological analysis revealed

- 500 1. Very low concentrations of hydrocarbons in the sediment.
- 501 2. Almost no depletion of porewater sulfate with depth.
- 502 3. Low sulfate reduction rates, close to detection limit.
- 503 4. Currently no anaerobic oxidation of methane in upper 3 mbsf.
- 504 5. No significant and consistent differences in any measured parameter
505 between sites inside and outside of pockmarks.

506 This indicates astonishingly low microbial activity in the study area, which supports
507 the assumption that currently no active fluid venting is taking place. Based on our
508 own findings and the current literature we hypothesize that the pockmark occurrence
509 and its formation is most likely related to a paleo-event during the last deglaciation.

510

511 **Acknowledgements**

512 We would like to thank LUNDIN Petroleum Norway for funding the research project
513 and providing the bathymetric data. GeolabNor AS is acknowledged for providing the
514 gas profile data. We thank the crew and shipboard scientific party of the R/V HU
515 Sverdrup and the shore-based staff of FFI and NGU for excellent support during the
516 expedition and Jan Erik Bjørøy and his crew from Fugro for coring. Ilya Ostanin is
517 thanked for assistance in the preparation of this paper. We acknowledge the two
518 anonymous reviewers and the editor for the constructive comments which helped to
519 improve this manuscript. This work contributed to the Helmholtz Climate Initiative
520 REKLIM.

521 **References**

522

- 523 Andreassen, K., Laberg, J.S., Vorren, T.O., 2008. Seafloor geomorphology of the SW Barents
524 Sea and its glaci-dynamic implications. *Geomorphology* 97, 157-177.
- 525 Berner, R.A., 1980. *Early Diagenesis: A Theoretical Approach*. Princeton University Press,
526 New Jersey.
- 527 Boetius, A., Ravensschlag, K., Schubert, C.J., Rickert, D., Widdel, F., Gieseke, A., Amann, R.,
528 Jorgensen, B.B., Witte, U., Pfannkuche, O., 2000. A marine microbial consortium
529 apparently mediating anaerobic oxidation of methane. *Nature* 407, 623-626.
- 530 Brothers, L., Kelley, J., Belknap, D., Barnhardt, W., Andrews, B., Maynard, M., 2011. More
531 than a century of bathymetric observations and present-day shallow sediment
532 characterization in Belfast Bay, Maine, USA: implications for pockmark field
533 longevity. *Geo-Marine Letters* 31, 237-248.
- 534 Cathles, L.M., Su, Z., Chen, D., 2010. The physics of gas chimney and pockmark formation,
535 with implications for assessment of seafloor hazards and gas sequestration. *Marine and*
536 *Petroleum Geology* 27, 82-91.
- 537 Cavanagh, A.J., Di Primio, R., Scheck-Wenderoth, M., Horsfield, B., 2006. Severity and
538 timing of Cenozoic exhumation in the southwestern Barents Sea. *Journal of the*
539 *Geological Society* 163, 761-774.
- 540 Chand, S., Mienert, J., Andreassen, K., Knies, J., Plassen, L., Fotland, B., 2008. Gas hydrate
541 stability zone modelling in areas of salt tectonics and pockmarks of the Barents Sea
542 suggests an active hydrocarbon venting system. *Marine and Petroleum Geology* 25,
543 625-636.
- 544 Chappellaz, J., Blunier, T., Raynaud, D., Barnola, J.M., Schwander, J., Stauffert, B., 1993.
545 Synchronous changes in atmospheric CH₄ and Greenland climate between 40 and 8
546 kyr BP. *Nature* 366, 443-445.
- 547 Cole, D., Stewart, S.A., Cartwright, J.A., 2000. Giant irregular pockmark craters in the
548 Palaeogene of the Outer Moray Firth Basin, UK North Sea. *Marine and Petroleum*
549 *Geology* 17, 563-577.
- 550 Corcoran, D.V., Dore, A.G., 2002. Depressurization of hydrocarbon-bearing reservoirs in
551 exhumed basin settings: evidence from Atlantic margin and borderland basins.
552 *Geological Society, London, Special Publications* 196, 457-483.
- 553 D'Hondt, S., Rutherford, S., Spivack, A.J., 2002. Metabolic Activity of Subsurface Life in
554 Deep-Sea Sediments. *Science* 295, 2067-2070.
- 555 Davy, B., Pecher, I., Wood, R., Carter, L., Gohl, K., 2010. Gas escape features off New
556 Zealand: Evidence of massive release of methane from hydrates. *Geophysical*
557 *Research Letters* 37, L21309.
- 558 Eidvin, T., Jansen, E., Riis, F., 1993. Chronology of Tertiary fan deposits off the western
559 Barents Sea: Implications for the uplift and erosion history of the Barents Shelf.
560 *Marine Geology* 112, 109-131.
- 561 Elverhøi, A., Andersen, E.S., Dokken, T., Hebbeln, D., Spielhagen, R., Svendsen, J.I.,
562 Sørflaten, M., Rørnes, A., Hald, M., Forsberg, C.F., 1995. The Growth and Decay of
563 the Late Weichselian Ice Sheet in Western Svalbard and Adjacent Areas Based on
564 Provenance Studies of Marine Sediments. *Quaternary Research* 44, 303-316.
- 565 Ferdelman, T.G., Fossing, H., Neumann, K., Schulz, H.D., 1999. Sulfate Reduction in Surface
566 Sediments of the Southeast Atlantic Continental Margin between 15°38'S and 27°57'S
567 (Angola and Namibia). *Limnology and Oceanography* 44, 650-661.
- 568 Ferrell, R.E., Aharon, P., 1994. Mineral assemblages occurring around hydrocarbon vents in
569 the northern Gulf of Mexico. *Geo-Marine Letters* 14, 74-80.

570 Finke, N., Vandieken, V., Jørgensen, B.B., 2007. Acetate, lactate, propionate, and isobutyrate
571 as electron donors for iron and sulfate reduction in Arctic marine sediments, Svalbard.
572 FEMS Microbiology Ecology 59, 10-22.

573 Forwick, M., Baeten, N.J., Vorren, T.O., 2009. Pockmarks in Spitsbergen fjords. Norwegian
574 Journal of Geology 89, 65-77.

575 Fossing, H., Ferdelman, T.G., Berg, P., 2000. Sulfate reduction and methane oxidation in
576 continental margin sediments influenced by irrigation (South-East Atlantic off
577 Namibia). *Geochimica et Cosmochimica Acta* 64, 897-910.

578 Foucher, J.-P., Westbrook, G.K., Boetius, A., Ceramicola, S., Dupre, S., Mascle, J., Mienert,
579 J., Pfannkuche, O., Pierre, C., Praeg, D., 2009. Structure and Drivers of Cold Seep
580 Ecosystems. *Oceanography* 22, 92-109.

581 Gabrielsen, R.H., Faereth, R.B., Jensen, L.N., Kalheim, J.E., Riis, F., 1990. Structural
582 elements of the Norwegian continental shelf, Part I: The Barents Sea Region. NPD-
583 Bulletin No. 6, 1-33.

584 Gay, A., Lopez, M., Berndt, C., Séranne, M., 2007. Geological controls on focused fluid flow
585 associated with seafloor seeps in the Lower Congo Basin. *Marine Geology* 244, 68-92.

586 Gay, A., Lopez, M., Cochonat, P., Levaché, D., Sermondadaz, G., Seranne, M., 2006.
587 Evidences of early to late fluid migration from an upper Miocene turbiditic channel
588 revealed by 3D seismic coupled to geochemical sampling within seafloor pockmarks,
589 Lower Congo Basin. *Marine and Petroleum Geology* 23, 387-399.

590 Hammer, Ø., Webb, K., Depreiter, D., 2009. Numerical simulation of upwelling currents in
591 pockmarks, and data from the Inner Oslofjord, Norway. *Geo-Marine Letters* 29, 269-
592 275.

593 Harrington, P., 1985. Formation of pockmarks by pore-water escape. *Geo-Marine Letters* 5,
594 193-197.

595 Hartwig, A., Anka, Z., di Primio, R., Albrecht, T., 2012. Evidence of a widespread paleo-
596 pockmarked field in the Orange Basin: An indication of an early Eocene massive fluid
597 escape event offshore South Africa. *Marine Geology*, this issue.

598 Hasiotis, T., Papatheodorou, G., Ferentinos, G., 2002. A string of large and deep gas-induced
599 depressions (pockmarks) offshore Killini peninsula, western Greece. *Geo-Marine*
600 *Letters* 22, 142-149.

601 Hovland, M., Gardner, J.V., Judd, A.G., 2002. The significance of pockmarks to
602 understanding fluid flow processes and geohazards. *Geofluids* 2, 127-136.

603 Hovland, M., Heggland, R., De Vries, M.H., Tjelta, T.I., 2010. Unit-pockmarks and their
604 potential significance for predicting fluid flow. *Marine and Petroleum Geology* 27,
605 1190-1199.

606 Hovland, M., Judd, A.G., 1988. Seabed pockmarks and Seepages. Impact on Geology,
607 Biology and the Marine Environment. Graham and Trotman, London.

608 Jørgensen, B.B., 1978. A Comparison of Methods for the Quantification of Bacterial Sulfate
609 Reduction in Coastal Marine Sediments I. Measurement with Radiotracer Techniques.
610 *Geomicrobiology Journal* 1, 11-26.

611 Jørgensen, B.B., 1982. Mineralization of organic matter in the sea bed-the role of sulphate
612 reduction. *Nature* 296, 643-645.

613 Jørgensen, B.B., Fenchel, T., 1974. The sulfur cycle of a marine sediment model system.
614 *Marine Biology* 24, 189-201.

615 Jørgensen, B.B., Weber, A., Zopfi, J., 2001. Sulfate reduction and anaerobic methane
616 oxidation in Black Sea sediments. *Deep Sea Research* 1 48, 2097-2120.

617 Judd, A., Hovland, M., 2007. Seabed Fluid Flow. The Impact on Geology, Biology, and the
618 Marine Environment. Cambridge University Press, New York.

619 Junttila, J., Aagaard-Sørensen, S., Husum, K., Hald, M., 2010. Late Glacial-Holocene clay
620 minerals elucidating glacial history in the SW Barents Sea. *Marine Geology* 276, 71-
621 85.

622 Kallmeyer, J., Ferdelman, T.G., Weber, A., Fossing, H., Jørgensen, B.B., 2004. A cold
623 chromium distillation procedure for radiolabeled sulfide applied to sulfate reduction
624 measurements. *Limnology and Oceanography: Methods* 2, 171-180.

625 King, L.H., MacLean, B., 1970. Pockmarks on the Scotian Shelf. *Geological Society of
626 America Bulletin* 81, 3141-3148.

627 Knittel, K., Boetius, A., 2009. Anaerobic Oxidation of Methane: Progress with an Unknown
628 Process. *Annual Review of Microbiology* 63, 311-334.

629 Kvenvolden, K.A., 1998. A primer on the geological occurrence of gas hydrate. *Geological
630 Society, London, Special Publications* 137, 9-30.

631 Lammers, S., Suess, E., Hovland, M., 1995. A large methane plume east of Bear Island
632 (Barents Sea): implications for the marine methane cycle. *Geologische Rundschau* 84,
633 59-66.

634 Larssen, G.B., Elvebakk, G., Henriksen Leif B., Kristensen, S.-E., Nilsson, I., Samuelsen,
635 T., Svånå, T.A., Stemmerik, L., Worsely, D., 2005. Upper Palaeozoic lithostratigraphy
636 of the southern Norwegian Barents Sea. *Geological Survey of Norway, Trondheim*.

637 Leloup, J., Loy, A., Knab, N.J., Borowski, C., Wagner, M., Jørgensen, B.B., 2007. Diversity
638 and abundance of sulfate-reducing microorganisms in the sulfate and methane zones
639 of a marine sediment, Black Sea. *Environmental Microbiology* 9, 131-142.

640 Long, D., 1992. Devensian late-glacial gas escape in the central North Sea. *Continental Shelf
641 Research* 12, 1097-1110.

642 Long, D., Lammers, S., Linke, P., 1998. Possible hydrate mounds within large sea-floor
643 craters in the Barents Sea. *Geological Society, London, Special Publications* 137, 223-
644 237.

645 Luff, R., Wallmann, K., 2003. Fluid flow, methane fluxes, carbonate precipitation and
646 biogeochemical turnover in gas hydrate-bearing sediments at Hydrate Ridge, Cascadia
647 Margin: numerical modeling and mass balances. *Geochimica et Cosmochimica Acta*
648 67, 3403-3421.

649 Martens, C.S., Berner, R.A., 1974. Methane Production in the Interstitial Waters of Sulfate-
650 Depleted Marine Sediments. *Science* 185, 1167-1169.

651 Maslin, M., Owen, M., Day, S., Long, D., 2004. Linking continental-slope failures and
652 climate change: Testing the clathrate gun hypothesis. *Geology* 32, 53-56.

653 Mienert, J., Posewang, J., Baumann, M., 1998. Gas hydrates along the northeastern Atlantic
654 margin: possible hydrate-bound margin instabilities and possible release of methane.
655 *Geological Society, London, Special Publications* 137, 275-291.

656 Niemann, H., Losekann, T., de Beer, D., Elvert, M., Nadalig, T., Knittel, K., Amann, R.,
657 Sauter, E.J., Schluter, M., Klages, M., Foucher, J.P., Boetius, A., 2006. Novel
658 microbial communities of the Haakon Mosby mud volcano and their role as a methane
659 sink. *Nature* 443, 854-858.

660 O'Connor, F.M., Boucher, O., Gedney, N., Jones, C.D., Folberth, G.A., Coppel, R.,
661 Friedlingstein, P., Collins, W.J., Chappellaz, J., Ridley, J., Johnson, C.E., 2010.
662 Possible role of wetlands, permafrost, and methane hydrates in the methane cycle
663 under future climate change: A review. *Reviews of Geophysics* 48, RG4005.

664 Ondréas, H., Olu, K., Fouquet, Y., Charlou, J., Gay, A., Dennielou, B., Donval, J., Fifis, A.,
665 Nadalig, T., Cochonat, P., Cauquil, E., Bourillet, J., Moigne, M., Sibuet, M., 2005.
666 ROV study of a giant pockmark on the Gabon continental margin. *Geo-Marine Letters*
667 25, 281-292.

668 Orphan, V.J., House, C.H., Hinrichs, K.-U., McKeegan, K.D., DeLong, E.F., 2001. Methane-
669 Consuming Archaea Revealed by Directly Coupled Isotopic and Phylogenetic
670 Analysis. *Science* 293, 484-487.

671 Paull, C., Ussler, W., Maher, N., Greene, H.G., Rehder, G., Lorenson, T., Lee, H., 2002.
672 Pockmarks off Big Sur, California. *Marine Geology* 181, 323-335.

673 Pimenov, N., Ulyanova, M., Kanapatsky, T., Veslopolova, E., Sigalevich, P., Sivkov, V.,
674 2010. Microbially mediated methane and sulfur cycling in pockmark sediments of the
675 Gdansk Basin, Baltic Sea. *Geo-Marine Letters* 30, 439-448.

676 Plaza-Faverola, A., Bünz, S., Mienert, J., 2012. The free gas zone beneath gas hydrate bearing
677 sediments and its link to fluid flow: 3-D seismic imaging offshore mid-Norway.
678 *Marine Geology*, available online, DOI: 10.1016/j.margeo.2011.07.002.

679 Prior, D.B., Doyle, E.H., Kaluza, M.J., 1989. Evidence for Sediment Eruption on Deep Sea
680 Floor, Gulf of Mexico. *Science* 243, 517-519.

681 Raghoebarsing, A.A., Pol, A., van de Pas-Schoonen, K.T., Smolders, A.J.P., Ettwig, K.F.,
682 Rijpstra, W.I.C., Schouten, S., Damste, J.S.S., Op den Camp, H.J.M., Jetten, M.S.M.,
683 Strous, M., 2006. A microbial consortium couples anaerobic methane oxidation to
684 denitrification. *Nature* 440, 918-921.

685 Reeburgh, W.S., 2007. Oceanic Methane Biogeochemistry. *Chemical Reviews* 107, 486-513.

686 Schippers, A., Köweker, G., Höft, C., Teichert, B.M.A., 2010. Quantification of Microbial
687 Communities in Forearc Sediment Basins off Sumatra. *Geomicrobiology Journal* 27,
688 170-182.

689 Siegert, M.J., Dowdeswell, J.A., Hald, M., Svendsen, J.-I., 2001. Modelling the Eurasian Ice
690 Sheet through a full (Weichselian) glacial cycle. *Global and Planetary Change* 31,
691 367-385.

692 Sloan, E.D., 2003. Fundamental principles and applications of natural gas hydrates. *Nature*
693 426, 353-363.

694 Solheim, A., Elverhøi, A., 1985. A pockmark field in the Central Barents Sea; gas from a
695 petrogenic source? *Polar Research* 3, 11-19.

696 Solheim, A., Elverhøi, A., 1993. Gas-related sea floor craters in the Barents Sea. *Geo-Marine*
697 *Letters* 13, 235-243.

698 Sultan, N., Marsset, B., Ker, S., Marsset, T., Voisset, M., Vernant, A.M., Bayon, G., Cauquil,
699 E., Adamy, J., Colliat, J.L., Drapeau, D., 2010. Hydrate dissolution as a potential
700 mechanism for pockmark formation in the Niger delta. *Journal of Geophysical*
701 *Research* 115, B08101.

702 Taniguchi, M., Burnett, W.C., Cable, J.E., Turner, J.V., 2002. Investigation of submarine
703 groundwater discharge. *Hydrological Processes* 16, 2115-2129.

704 Treude, T., Boetius, A., Knittel, K., Wallmann, K., Jørgensen, B.B., 2003. Anaerobic
705 oxidation of methane above gas hydrates at Hydrate Ridge, NE Pacific Ocean. *Marine*
706 *Ecology Progress Series* 264, 1-14.

707 Treude, T., Krüger, M., Boetius, A., Jørgensen, B.B., 2005a. Environmental Control on
708 Anaerobic Oxidation of Methane in the Gassy Sediments of Eckernförde Bay (German
709 Baltic). *Limnology and Oceanography* 50, 1771-1786.

710 Treude, T., Niggemann, J., Kallmeyer, J., Wintersteller, P., Schubert, C.J., Boetius, A.,
711 Jørgensen, B.B., 2005b. Anaerobic oxidation of methane and sulfate reduction along
712 the Chilean continental margin. *Geochimica et Cosmochimica Acta* 69, 2767-2779.

713 Ussler, W., Paull, C.K., Boucher, J., Friederich, G.E., Thomas, D.J., 2003. Submarine
714 pockmarks: a case study from Belfast Bay, Maine. *Marine Geology* 202, 175-192.

715 Vaular, E.N., Barth, T., Haflidason, H., 2010. The geochemical characteristics of the hydrate-
716 bound gases from the Nyegga pockmark field, Norwegian Sea. *Organic Geochemistry*
717 41, 437-444.

- 718 Vorren, T.O., Laberg, J.S., 1996. Late glacial air temperature, oceanographic and ice sheet
719 interactions in the southern Barents Sea region. Geological Society, London, Special
720 Publications 111, 303-321.
- 721 Webb, K., Hammer, Ø., Lepland, A., Gray, J., 2009. Pockmarks in the inner Oslofjord,
722 Norway. Geo-Marine Letters 29, 111-124.
- 723 Weber, A., Riess, W., Wenzhoefer, F., Jørgensen, B.B., 2001. Sulfate reduction in Black Sea
724 sediments: in situ and laboratory radiotracer measurements from the shelf to 2000 m
725 depth. Deep Sea Research Part I: Oceanographic Research Papers 48, 2073-2096.
- 726 Whiticar, M., Werner, F., 1981. Pockmarks: Submarine vents of natural gas or freshwater
727 seeps? Geo-Marine Letters 1, 193-199.
- 728 Whiticar, M.J., 2002. Diagenetic relationships of methanogenesis, nutrients, acoustic
729 turbidity, pockmarks and freshwater seepages in Eckernförde Bay. Marine Geology
730 182, 29-53.
- 731 Woolsey, T.S., McCallum, M.E., Schumm, S.A., 1975. Modeling of diatreme emplacement
732 by fluidization. Physics and Chemistry of The Earth 9, 29-42.
- 733
- 734